

Raffalt, P. C., Senderling, B., Stergiou, N. (2020). Filtering affects the calculation of the largest Lyapunov exponent. *Computers in Biology and Medicine*, 122, Artikkel 103786.  
10.1016/j.combiomed.2020.103786

---

Dette er siste tekst-versjon av artikkelen, og den kan inneholde små forskjeller fra forlagets pdf-versjon. Forlagets pdf-versjon finner du her:  
<http://dx.doi.org/10.1016/j.combiomed.2020.103786>

---

This is the final text version of the article, and it may contain minor differences from the journal's pdf version. The original publication is available here:  
<http://dx.doi.org/10.1016/j.combiomed.2020.103786>

---

## ORIGINAL RESEARCH STUDY

### Title

Filtering affects the calculation of the Largest Lyapunov Exponent

### Authors

Peter C. Raffalt<sup>1,2</sup>, Benjamin Senderling<sup>2</sup> and Nick Stergiou<sup>2,3</sup>

### Affiliations:

1 Institute of Physical Performance, Norwegian School of Sport Sciences, Sognsveien  
220, 0806 Oslo, Norway.

2 Department of Biomechanics and Center for Research in Human Movement  
Variability, University of Nebraska at Omaha, 6160 University Drive, Omaha, NE 68182-  
0860, USA.

3 College of Public Health, 984355 University of Nebraska Medical Center, Omaha, NE  
68198-4355, USA.

### Corresponding Author:

Nick Stergiou, PhD

Department of Biomechanics and Center for Research in Human Movement Variability

University of Nebraska at Omaha

6160 University Drive

Omaha, NE 68182-0860, USA.

Email: [nstergiou@unomaha.edu](mailto:nstergiou@unomaha.edu)

Phone: 402-554-3247

## Abstract

The calculation of the largest Lyapunov exponent (LyE) requires the reconstruction of the time series in an N-dimensional state space. For this, the time delay (Tau) and embedding dimension (EmD) are estimated using the Average Mutual Information and False Nearest Neighbor algorithms. However, the estimation of these variables (LyE, Tau, EmD) could be compromised by prior filtering of the time series evaluated. Therefore, we investigated the effect of filtering kinematic marker data on the calculation of Tau, EmD and LyE using several different computational codes. Kinematic marker data were recorded from 37 subjects during treadmill walking and filtered using a low pass digital filter with a range of cut-off frequencies (23.5–2Hz). Subsequently, the Tau, EmD and LyE were calculated from all cut-off frequencies. Our results demonstrated that the level of filtering affected the outcome of the Tau, EmD and LyE calculations for all computational codes used. However, there was a more consistent outcome for cut-off frequencies above 10 Hz which corresponded to the optimal cut-off frequency that could be used with this data. This suggested that kinematic data should remain unfiltered or filtered conservatively before calculating Tau, EmD and LyE.

**Keywords:** nonlinear analysis, cut-off frequency, walking, smoothing, biomechanics

## Introduction

In traditional evaluation of biomedical and in particular biomechanical data, peaks or means or other points of interests are often extracted from the trajectories of the parameters of interest [1]. Subsequently, they are averaged across multiple movement cycles. However, before calculating these parameters and extracting the values of these points, the recorded time series are often filtered using a digital filter to remove potential noise. This is especially true in the evaluation of kinematics data in gait analysis due to movements in the markers placed on the subject's skin [2-6]. However, filtering a biological signal includes also the risk of removing relevant information [7]. This could be particularly important when nonlinear dynamics methods are used for further analysis [8, 9]. Such methods have gained great interest and popularity in recent years [7, 9-12]. Common for these methods is the appreciation and quantification of the time dependency in the trajectories of the parameters in question [7-12]. Therefore, any kind of temporal manipulation, due to filtering and/or interpolation, could potentially affect this time dependency.

One nonlinear dynamics method that is gaining popularity in biomechanics research is the evaluation of the largest Lyapunov exponent (LyE). This is especially true in gait analysis where a recent search on PubMed using *Lyapunov* and *gait* as keywords, returned 167 results. The LyE measures the exponential divergence of the movement trajectories within the reconstructed state space [13]. State space reconstruction is a nonlinear dynamics technique that uses a time delay to create  $M$  copies of the original time series, where  $M$  is the embedding dimension. LyE has often been applied to kinematic data such as the center of mass acceleration [14-17] and joint

angle [14-16, 18] time series recorded during walking which are characterized by a limited cycle attractor behavior. The LyE has the advantage of measuring the divergence of cycles within the attractor, thus, quantifying the stride-to-stride variability in the inherently periodic time series [19]. Such information could allow us to identify how stable walking is across different experimental groups as well as to discern the effect of various pathologies.

The calculation of LyE requires the reconstruction of the state space based on a carefully identified time lag ( $\tau$ ) and an embedding dimension ( $m$ ). Recently, Mehdizadeh and Sanjari showed that time series filtering can affect the outcome of the LyE calculation in a time series derived from a passive dynamic walker [20]. However, it is unknown how filtering of actual biological data could affect the estimation of  $\tau$ ,  $m$  and LyE. In the present study, these ideas have been expanded using several different computational codes and algorithms to calculate  $\tau$  and LyE from biological data [21-23]. Thomas et al. (2014) compared eight different computational codes to calculate  $\tau$  and observed considerable differences in the outcome [22]. Similarly, Cignetti et al. (2012), Raffalt et al. (2018) and Raffalt et al. (2019) have observed differences in the outcomes when applying the two most commonly used algorithms (the Rosenstein et al. algorithm [24] and the Wolf et al. algorithm [13]) to estimate the LyE from the same gait data [21, 23, 25].

Therefore, in the present study we investigated the effect of data filtering on the calculation of  $\tau$ ,  $m$  and LyE. To achieve this aim, gait kinematics recorded from healthy individuals walking at their self-selected speed was filtered with a range of cut off frequencies previously used in the literature [26]. It was hypothesized that relatively

low cut-off frequencies would remove both unwanted noise and relevant information, thereby changing significantly the outcome of the Tau, EmD and LyE calculations as compared to unfiltered data.

To further enhance the generalizability of our efforts, we included five computational codes of the Tau calculation, two different algorithms for the LyE calculation (the Rosenstein et al. algorithm [24] and the Wolf et al. algorithm [13]), and three different computational codes specifically for the Wolf et al. algorithm. Additionally, since the filtering cut-off frequency for gait data can be determined using the approach presented by Yu and colleagues [27], we calculated this optimal cut-off frequency from our data to clarify how this methodological choice compares with our results. Lastly, we applied the above algorithms on gait kinematic data and specifically on the hip, knee, and ankle angles. This further allowed us to investigate if using different algorithms could affect the inter-joint relationship of each investigated variable.

## Materials and Methods

### Participants

Thirty-seven healthy older males (age:  $65.6 \pm 9.7$  years; body height:  $1.75 \pm 0.08$  m; body mass:  $78.6 \pm 16.0$  kg) were recruited for the present study. Participants were without neurological disorders or lower limb injuries that could affect their gait. All participants provided informed written consent prior to participation. The study was approved by the Institutional Review Board of the University of Nebraska Medical Center and the study was carried out in accordance with the approved guidelines.

### Experimental setup

Upon arrival to the laboratory, the participants were fitted with 33 reflective markers placed bilaterally on: anterior superior iliac spines, posterior superior iliac spines, greater trochanters, midlateral thighs, lower front thighs, lateral and medial condyles, tibial tubercles, lower lateral shanks, lateral and medial malleolus, distal end of the second metatarsophalangeal (MTP) joints, posterior heels, distal lateral fifth MTPs, and lateral calcanei. An additional single marker was placed on the sacrum. After recording a calibration posture for Visual3D (C-Motion, Germantown, USA), six medial markers were removed. Prior to any data collection, the self-selected preferred treadmill walking speed of each participant was established. This was accomplished by increasing and decreasing the speed of the instrumented treadmill (DBCEEWI-1, AMTI, Watertown, USA) above and below what the participants reported as being comfortable. On average, the preferred speed was  $1.04 \pm 0.24$  m/s. The participants then continued to walk for three minutes at their self-selected preferred speed during which the three-

dimensional position data were recorded by a 12 high-speed infrared camera motion capture system (Motion Analysis Corporation, Rohnert Park, USA) operating at 60 Hz.

## Data analysis

The data analysis process is schematically presented in Figure 1. The raw marker position data was filtered iteratively using a fourth order Butterworth filter from 23.5 Hz to 2 Hz in decrements of 0.5 [26]. For each iteration, the filtered data was used to calculate joint angles in Visual3D. The bilateral model used to calculate joint angles is described in the supplementary material. The optimal cut-off frequency was calculated from the position data using the equation presented by Yu and colleagues [27]. Subsequently, it was averaged across markers and subjects, and was found to be 10.9 Hz.

Sagittal hip, knee and ankle joint angles of the left leg were calculated for the unfiltered data and 44 different filtered versions of the data. The time series was also truncated to 178 seconds (10680 data points). To investigate the main frequency of oscillation in the investigate time series, spectral density analyses were performed on representative hip, knee and ankle joint angle time series from one subject.

Tau was calculated using the Average Mutual Information algorithm [28-30]. This algorithm calculates the probability that the information within time-delayed copies of the original time series is different (Equation 1) [29].

$$\text{Equation 1: } I(k) = \sum_{t=1}^n P(x_t, x_{t+k}) \log_x \frac{P(x_t, x_{t+k})}{P(x_t)P(x_{t+k})}$$

where  $I$  is the mutual average information and  $k$  is the time delay.

With each time delay tested, the proper delay is determined as the first local minimum in the probability. EmD was calculated using the False Nearest Neighbor algorithm [29,

31]. This procedure includes the creation of multiple time-delayed copies of the original time series where the percentage of ‘false nearest neighbors’ is subsequently calculated. A false nearest neighbor is identified as a point that appears close in lower dimensions but whose distance increases above a critical value when the time series is unfolded to a higher dimension (Equation 2).

$$\text{Equation 2: } \frac{\|\hat{V}(t) - \hat{V}^{NN}(t)\| - \|V(t) - V^{NN}(t)\|}{\|V(t) - V^{NN}(t)\|} > R_{tol}$$

where  $V(t)$  is the state vector of a given dimension,  $V^{NN}(T)$  is the state vector of the nearest neighbor,  $\hat{\phantom{x}}$  indicates a higher dimension and  $R_{tol}$  is the critical limit.

The proper dimension is determined as the dimension at which the percentage of false nearest neighbors drops to zero [29]. For the Tau calculations, five different computational codes were used (Richardson, Richardson128, Stergiou, Stergiou128 and Thomas; for details, see Table 1). Due to processing constraints, only the first 1000 data points of each time series were used in the Thomas code. Using the Tau calculated with the Thomas code (Table 1) and the EmD, each time series was reconstructed in state space (Equations 3).

$$\text{Equation 3: } y(t) = [x(t), x(t + \tau), x(t + 2\tau), \dots, x(t + (M - 1)\tau)]$$

Where  $y(t)$  is the  $M$ -dimensional coordinates for the reconstructed point at time  $t$  derived from original data point  $x(t)$ .

Subsequently, the LyE was calculated using the Rosenstein et al. algorithm [24] with a custom made Matlab script and the Wolf et al. algorithm [13] using three different computational codes (see Table 1 for details and supplementary material for codes). The calculation procedures of the LyE using the two algorithms have been described in details elsewhere and briefly below [21, 25]. Both algorithms quantify the exponential

rate of divergence or convergence of nearest neighboring data points on an attractor over time. The Wolf et al. algorithm [13] uses a reference trajectory and follows one nearest neighboring data point until the distance to the reference trajectory exceeds a predefined limit at which the nearest neighbor data point is replaced. In the present study, this limit was set at one tenth the range of the data. Replacements are found excluding those within a minimum distance of  $1e-4$  and outside an angle of  $30^\circ$  to the reference trajectory. These secondary parameters to the LyE codes were consistent between all three codes. The average  $\log_2$  of increasing/decreasing distance between compared data points is divided by the time the data pair was followed until the nearest neighbor was replaced (Equation 4).

$$\text{Equation 4: } Z_1 = \frac{(\log_2 \frac{L'(t_1)}{L(t_0)})}{(dt \times n)}$$

where  $Z$  is the exponential divergence/convergence,  $L'(t_1)$  is the Euclidian distance between vectors after time evolution and  $L(t_0)$  is the initial distance between vectors.

The Rosenstein et al. algorithm [24] plots the log of the Euclidian distances between neighboring data points as a function of a predetermined time period. This is completed for all pairs of neighboring data points and a mean ensemble curve is calculated. The rate of divergence or convergence is reported as the average natural log of the increasing/decreasing distance from the Wolf et al. algorithm [13] and the slope of a linear fit across the increasing region of the mean curve (zero to 0.5 strides) from the Rosenstein et al. algorithm [24]. All calculations were carried out in Matlab (Mathworks R2011, Inc., Natick, MA). To increase the processing speed of the calculations, the data was de-identified and the scripts were run using the Holland Computing Center's Tusker

supercomputer located at the Peter Kiewit Institute of the University of Nebraska at Omaha campus.

## **Statistics**

A total of 4995 time series (37 subjects x 3 joints x 45 cut-off frequencies) were extracted and the following variables were calculated from each time series: 1 EmD, 5 different Tau and 4 different LyE (Figure 1). To investigate the effect of joint angle, cut-off frequency, and their interaction (joint angle x cut-off frequency), a two-way ANOVA with repeated measures was utilized with 3 levels of joint angles and 45 levels of cut-off frequencies as the independent factors. Thus, in total 10 (1 EmD, 5 Tau, 4 LyE) ANOVAs were conducted. In case of an overall significant effect of the independent factors or the interaction, a Holm-Sidak post hoc test was utilized. The level of significance was set a 0.05. All statistical analyses were performed in SPSS (IBM, SPSS Statistics, version 24, NY, USA).

## Results

### Spectral density

The spectral density analysis revealed a peak in power spectral density for the hip joint angle at 1 Hz, two peaks for the knee joint around 1 Hz and just below 2 Hz and three peaks for the ankle joint around 1 Hz, just below 2 Hz and at approximately 2,7 Hz (Figure 1).

### Time delay (Tau)

When using the five different codes to calculate Tau, there was a significant effect of joint (Richardson:  $F = 17.7$ ,  $p < 0.001$ ; Richardson128:  $F = 39.7$ ,  $p < 0.001$ ; Stergiou:  $F = 36.9$ ,  $p < 0.001$ ; Stergiou128:  $F = 37.2$ ,  $p < 0.001$ ; and Thomas:  $F = 43.2$ ,  $p < 0.001$ , respectively), cut-off frequency (Richardson:  $F = 2.6$ ,  $p < 0.001$ ; Richardson128:  $F = 1.4$ ,  $p = 0.035$ ; Stergiou:  $F = 4.4$ ,  $p < 0.001$ ; Stergiou128:  $F = 1.5$ ,  $p < 0.014$ , and Thomas:  $F = 3.9$ ,  $p < 0.001$ , respectively) as well as a significant interaction (Richardson:  $F = 2.5$ ,  $p < 0.001$ ; Richardson128:  $F = 2.6$ ,  $p < 0.001$ ; Stergiou:  $F = 2.2$ ,  $p < 0.001$ ; Stergiou128:  $F = 2.7$ ,  $p < 0.001$ ; and Thomas:  $F = 5.8$ ,  $p < 0.001$ , respectively). For both unfiltered and filtered data, the Tau was significantly higher for the hip joint angle as compared to the knee and ankle joint angles for all five codes except for the Richardson code at cut-off frequencies below 3Hz (Figure 3). There was a significant difference in Tau between the knee and ankle joint angles, at lower cut-off frequencies. Specifically, this was the case for the Richardson code between 5 and 3 Hz, for the Richardson128 code below 4.5 Hz, for the Stergiou code below 6 Hz, for the Stergiou128 code below 4.5 Hz and for the Thomas code below 11 Hz. The five Tau codes exhibited a similar pattern for the three joints across the range

of cut-off frequencies (Figure 3). For the hip joint angle, the Tau did not change for the unfiltered and filtered data, except for the Richardson code where the Tau decreased at cut-off frequencies below 3 Hz. For the knee joint angle, the Tau was unchanged for all cut-off frequencies except at 2 Hz where it increased. For the ankle joint angle, the Tau locally decreased at cut-off frequencies between 6 and 2.5 Hz (Figure 3).

### **Embedding dimension (EmD)**

There was a significant effect of joint ( $F = 36.5$ ,  $p < 0.001$ ), cut-off frequency ( $F = 4.7$ ,  $p < 0.001$ ) and an interaction ( $F = 2.6$ ,  $p < 0.001$ ) on the calculated EmD. For both unfiltered and filtered data, the EmD was significantly lower for the hip joint angle compared to the knee and ankle joint angles. The EmD for the knee joint angle was significantly lower compared to the ankle joint for the unfiltered data. This difference was not consistent across all the cut-off frequencies (Figure 2). While the EmD of the hip and knee joint angles did not change with altered filtering, EmD significantly decreased for the ankle joint at cut-off frequencies below 3.5 Hz (Figure 2).

### **The largest Lyapunov exponent (LyE)**

When calculating LyE with the Rosenstein et al. algorithm (Cignetti code), there was a significant effect of joint ( $F = 4.8$ ,  $p = 0.011$ ), cut-off frequency ( $F = 59.2$ ,  $p < 0.001$ ) and an interaction ( $F = 7.9$ ,  $p < 0.001$ ). The knee joint angle had significantly higher LyE compared to the hip and ankle joint angles for the unfiltered data and the data filtered with a cut-off frequency between 23.5 and 7.5 Hz. No difference in LyE was observed between the hip and ankle joint angles (Figure 4). For the three codes of the Wolf et al. algorithm, the Knarr and Wurdeman code exhibited a similar pattern across the three joints and cut-off frequencies. There was a significant effect of joint ( $F = 41.0$ ,

$p < 0.001$  and  $F = 79.2$ , respectively), cut-off frequency ( $F = 32.7$ ,  $p < 0.001$  and  $F = 33.4$ ,  $p < 0.001$ , respectively) as well as a significant interaction ( $F = 19.7$ ,  $p < 0.001$  and  $F = 17.4$ ,  $p < 0.001$ , respectively). For both unfiltered and filtered data, the ankle joint exhibited significantly higher LyE as compared to the two proximal joints. No difference in LyE was observed between the knee and hip joint. The LyE decreased significantly at cut-off frequencies below 7.5 Hz. For the Wolf et al. algorithm using the Wolf code, there was a significant effect of joint ( $F = 29.2$ ,  $p < 0.001$ ), cut-off frequency ( $F = 2.3$ ,  $p < 0.001$ ) as well as a significant interaction ( $F = 1.3$ ,  $p = 0.048$ ). The calculated LyE of the knee joint angle was significantly higher as compared to the hip and ankle joint. Furthermore, a small but significant difference in LyE was observed between the hip and knee joint angle. However, this result was not consistent across all cut-off frequencies (Figure 4). Only the LyE of the ankle joint angle was affected by the altered cut-off frequency and decreased significantly at frequencies below 3 Hz.

## Discussion

In the present study, we investigated the effect of filtering gait kinematic data on the calculation of Tau, EmD and LyE of the lower limb joint angles. We included a range of cut-off frequencies, multiple computation codes for the Tau calculation and two commonly used algorithms for the LyE calculation (i.e. the Rosenstein et al. [24] and the Wolf et al. [13] algorithm). We hypothesized that filtering with relatively low cut-off frequencies would remove both unwanted noise and relevant information affecting the calculation of EmD, Tau and LyE. This hypothesis was confirmed as almost all investigated variables were significantly affected when low cut-off frequencies were used as compared to unfiltered and less filtered data. The optimal cut-off frequency of the included data was found to be 10.9 Hz and the spectral density analysis revealed that the peaks in the power spectral density for all three joint time series were well below 10 Hz.

The Tau calculations exhibited a similar inter-joint relationship across the five codes. The Tau of the hip joint was significantly higher as compared to the Tau of the knee and ankle joint. There were no differences in Tau between the two distal joints for unfiltered data and for filtered data with high cut-off frequencies. Similar to the EmD calculations, the inter-joint relationship changed at lower cut-off frequencies and the Tau increased or decreased significantly. This would support the use of either unfiltered data or high cut-off frequencies for the calculation of Tau. Based upon a visual inspection of the results from the different algorithms, we observed that the Richardson128, Stergiou128 and Thomas codes resulted in fewer fluctuations in the calculated EmD at various frequencies as compared to the Richardson and Stergiou codes. Recently,

Thomas and colleagues introduced the Thomas code to calculate the Average Mutual Information to estimate the time delay. They found that this code outperforms several other alternative codes [22]. Thus, considering all the above it is recommended that the Thomas algorithm should be favored for calculating Tau.

For the calculation of EmD, the inter-joint relationship between the hip joint and the two more distal joints was unaffected for the range of applied cut-off frequencies. In contrast, the inter-joint relationship of EmD between the knee and ankle joint appeared to be frequency dependent. A stable inter-joint relationship was observed for filtered data with cut-off frequencies between 22.5 – 14.5 Hz, where the EmD of the ankle joint was consistently higher than the EmD of the knee joint. The unfiltered data also showed a significant difference in EmD between the knee and ankle joint. Additionally, as cut-off frequency decreased, the EmD of the ankle joint decreased. This result suggested that lower cut-off frequencies could result in invalid outcomes. Therefore, calculation of EmD should be conducted on unfiltered data or with the application of relatively high cut-off frequencies.

Regarding the LyE calculations, the Rosenstein et al. algorithm using the Cignetti code and the Wolf et al. algorithm using the Wolf code returned a LyE value for the knee joint that was significantly higher than the hip and the ankle joint. In contrast, the Wolf et al. algorithm using the Knarr code or the Wurdeman code returned a LyE value for the ankle joint that was significantly higher than the hip and the knee joint. These observations seem to be in agreement with previous comparisons between the Rosenstein et al. and Wolf et al. algorithms applied to lower limb joint angles during walking [21, 23]. The difference in the absolute value of the LyE between the two

algorithms could be originated from the choice of several input parameters that are embedded in its calculation (e.g. the slope region, the nearest neighbor distance limit and the time series normalization [23, 25, 32]) or possibly in the organization of the algorithm within the code written by different individuals. While the Cignetti, Knarr and Wurdeman codes seemed to provide different results for cut-off frequencies below 10 Hz, the Wolf code showed an inconsistent inter-joint relationship between the hip and ankle joints. Practically, small increases or decreases in cut-off frequencies could lead to a significant difference in the LyE between the two joints. This would support the use of the former scripts and of unfiltered data or at least relatively high cut-off frequencies. This is agreement with a recent study by Mehdizadeh and Sanjari [20], who applied Gaussian white noise to a time series generated by a passive walker. These authors proposed that high cut-off frequencies rather than low frequencies should be applied to experimental data to purely eliminate unwanted high frequency noise. Interestingly, while the LyE values from the Rosenstein et al. algorithm increased for the three joints at low cut-off frequencies, the LyE values from the three codes of the Wolf et al. algorithm decreased at low cut-off frequencies. Ideally, filtering a biological signal removes unwanted noise and leaves only relevant information. However, the smoothing of a signal unavoidably removes detailed fluctuations of biological importance. Intuitively, such a process should reduce the exponential rate of the trajectory's divergence in state space. Surprisingly, this was the case for the Wolf et al. algorithm but not for the Rosenstein et al. algorithm. This could question the validity of the Rosenstein et al. algorithm when using data that are filtered at low cut-off frequencies. Recently, Mehdizadeh [33] presented a revised version of the Rosenstein et al.

algorithm which provided more consistent results in LyE estimation from both theoretical data (Lorenz attractor and passive walker) and biological data (3-dimensional kinematic data from walking). It is unknown, if the inclusion of this new algorithm would have altered the results of the present study and this issue needs to be addressed in subsequent experimental work.

It should be mentioned that in the present study, healthy elderly individuals were recruited and thus, their values of the EmD, Tau and LyE are potentially different from those of younger individuals. However, it is unlikely that using healthy young participants would have altered the overall conclusion or recommendations of the present study.

In general, a limited effect of filtering the data at high cut-off frequencies, as compared to unfiltered data, was observed in the present study. This could indicate that the calculation of joint angles from the raw kinematic data introduces a smoothing effect and additional filtering is redundant. While this seems to be true for joint movements during walking, this is not necessarily true for other tasks and movements, which calls for future studies.

In conclusion, the results of the present study suggest that future studies calculating Tau, EmD and LyE from lower limb joint angles during walking should use either unfiltered kinematic data or filtered data with a high cut-off frequency. Such a frequency should be above the calculated optimal cut-off frequency which in the present study was 10.9 Hz. Furthermore, the results of the present study recommend the usage of the Richardson128, Stergiou128 or the Thomas code for Tau calculations and the Cignetti, Knarr or Wurdeman code for the LyE calculations. All the Matlab codes are

available in the supplementary material for future studies performed in this growing area of research in biomechanics and motor control.

## **Acknowledgement**

The authors would like to thank the Holland Computing Center (<https://hcc.unl.edu>) for access their supercomputer and assistance in implementing the included computational codes. This study was supported by the Center for Research in Human Movement Variability and the NIH (P20GM109090, R15AG063106, and R01NS114282).

## **Conflict of interest**

None declared.

## References

- [1] M. Roberts, D. Mongeon, F. Prince, Biomechanical parameters for gait analysis: a systematic review of healthy human gait, *Physical Therapy and Rehabilitation*, 4 (2017) 6.
- [2] C.L. Vaughan, B.L. Davis, J.C. O'Conner, *Dynamics of Human Gait*, 1st ed., Human Kinetics 1992.
- [3] D.A. Winter, *Biomechanics and motor control of human movement*, John Wiley & Sons, Inc., Hoboken, New Jersey, USA, 2009.
- [4] D.L. Benoit, D.K. Ramsey, M. Lamontagne, L. Xu, P. Wretenberg, P. Renstrom, Effect of skin movement artifact on knee kinematics during gait and cutting motions measured in vivo, *Gait & posture*, 24 (2006) 152-164.
- [5] A. Leardini, L. Chiari, U. Della Croce, A. Cappozzo, Human movement analysis using stereophotogrammetry. Part 3. Soft tissue artifact assessment and compensation, *Gait & posture*, 21 (2005) 212-225.
- [6] W.R. Taylor, R.M. Ehrig, G.N. Duda, H. Schell, P. Seebeck, M.O. Heller, On the influence of soft tissue coverage in the determination of bone kinematics using skin markers, *Journal of orthopaedic research : official publication of the Orthopaedic Research Society*, 23 (2005) 726-734.
- [7] H. Kantz, T. Schreiber, *Nonlinear Time Series Analysis*, Cambridge University Press, Cambridge, UK, 2004.
- [8] P.E. Rapp, A guide to dynamical analysis, *Integr Physiol Behav Sci*, 29 (1994) 311-327.
- [9] N. Stergiou, *Innovative Analyses of Human Movement*, Human Kinetics, Champaign, Illinois USA, 2004.
- [10] N. Stergiou, *Nonlinear Analysis for Human Movement Variability*, Taylor & Francis Group, Boca Raton, Florida USA, 2016.
- [11] M. Shelhamer, *Nonlinear Dynamics in Physiology*, World Scientific Publishing Company, Singapore, 2006.
- [12] S.H. Strogatz, *Nonlinear dynamics and chaos : with applications to physics, biology, chemistry, and engineering*, Second edition ed., Westview Press, a member of the Perseus Books Group, Boulder, CO, 2015.
- [13] A. Wolf, J.B. Swift, H.L. Swinney, J.A. Vastano, Determining Lyapunov Exponents from a Time-Series, *Physica D*, 16 (1985) 285-317.
- [14] J.B. Dingwell, J.P. Cusumano, P.R. Cavanagh, D. Sternad, Local dynamic stability versus kinematic variability of continuous overground and treadmill walking, *Journal of biomechanical engineering*, 123 (2001) 27-32.
- [15] J.B. Dingwell, J.P. Cusumano, Nonlinear time series analysis of normal and pathological human walking, *Chaos*, 10 (2000) 848-863.
- [16] P.C. Raffalt, M.K. Guul, A.N. Nielsen, S. Puthusserypady, T. Alkjaer, Economy, Movement Dynamics, and Muscle Activity of Human Walking at Different Speeds, *Scientific reports*, 7 (2017) 43986.
- [17] S.M. Bruijn, J.H. van Dieen, O.G. Meijer, P.J. Beek, Is slow walking more stable?, *Journal of biomechanics*, 42 (2009) 1506-1512.
- [18] S.A. England, K.P. Granata, The influence of gait speed on local dynamic stability of walking, *Gait & posture*, 25 (2007) 172-178.
- [19] S.R. Wurdeman, S.A. Myers, A.L. Jacobsen, N. Stergiou, Prosthesis preference is related to stride-to-stride fluctuations at the prosthetic ankle, *Journal of Rehabilitation Research and Development*, 50 (2013) 671-686.
- [20] S. Mehdizadeh, M.A. Sanjari, Effect of noise and filtering on largest Lyapunov exponent of time series associated with human walking, *Journal of biomechanics*, 64 (2017) 236-239.

- [21] F. Cignetti, L.M. Decker, N. Stergiou, Sensitivity of the Wolf's and Rosenstein's algorithms to evaluate local dynamic stability from small gait data sets, *Annals of biomedical engineering*, 40 (2012) 1122-1130.
- [22] R.D. Thomas, N.C. Moses, E.A. Semple, A.J. Strang, An efficient algorithm for the computation of average mutual information: Validation and implementation in Matlab, *Journal of Mathematical Psychology*, 61 (2014) 45-59.
- [23] P. Raffalt, T. Alkjaer, B. Brynjolfsson, J.R. L, C.R. Bartholdy, M. Henriksen, Test-retest reliability of non-linear methods to assess walking dynamics, *Journal of biomechanical engineering*, (2018).
- [24] M.T. Rosenstein, J.J. Collins, C.J. De Luca, A practical method for calculating largest Lyapunov exponents from small data sets, *Physica D: Nonlinear Phenomena*, 65 (1993) 117-134.
- [25] P.C. Raffalt, J.A. Kent, S.R. Wurdeman, N. Stergiou, Selection Procedures for the Largest Lyapunov Exponent in Gait Biomechanics, *Annals of biomedical engineering*, 47 (2019) 913-923.
- [26] J. Sinclair, P.J. Taylor, S.J. Hobbs, Digital filtering of three-dimensional lower extremity kinematics: an assessment, *Journal of human kinetics*, 39 (2013) 25-36.
- [27] B. Yu, D. Gabriel, L. Noble, K.-N. An, Estimate of the Optimum Cutoff Frequency for the Butterworth Low-Pass Digital Filter, *Journal of Applied Biomechanics*, 15 (1999) 318-329.
- [28] F. Takens, Detecting strange attractors in turbulence, *Dynamical Systems and Turbulence, Lecture Notes in Mathematics*, 898 (1981) 366-381.
- [29] S.R. Wurdeman, State-Space Reconstruction, in: N. Stergiou (Ed.) *Nonlinear Analysis for Human Movement Variability*, Taylor & Francis Group, Boca Raton, Florida USA, 2016.
- [30] T. Sauer, J.A. Yorke, How many delay coordinates do you need?, *Int J Bifurc Chaos*, 3 (1993) 737-744.
- [31] T. Sauer, J.A. Yorke, M. Casdagli, Embedology, *J Stat Phys*, 65 (1991) 579-616.
- [32] J. Stenum, S.M. Bruijn, B.R. Jensen, The effect of walking speed on local dynamic stability is sensitive to calculation methods, *Journal of biomechanics*, 47 (2014) 3776-3779.
- [33] S. Mehdizadeh, A robust method to estimate the largest Lyapunov exponent of noisy signals: A revision to the Rosenstein's algorithm, *Journal of biomechanics*, 85 (2019) 84-91.
- [34] M.B. Kennel, R. Brown, H.D. Abarbanel, Determining embedding dimension for phase-space reconstruction using a geometrical construction, *Physical review. A, Atomic, molecular, and optical physics*, 45 (1992) 3403-3411.
- [35] C.A. Coey, M. Richardson, *Recurrence Analysis Toolbox*. Available from: <http://xkiwilabs.com/software-toolboxes>, 2013.
- [36] A. Leontitsis, *Mutual Average Information*. Available from: <https://www.mathworks.com/matlabcentral/fileexchange/880-mutual-average-information>, 2004.
- [37] D.W. Scott, Sturges' rule, *WIREs Computational Statistics*, 1 (2009) 303-306.
- [38] D.W. Scott, On optimal and data-based histograms, *Biometrika*, 66 (1979) 605-610.
- [39] A.S. Lanier, B.A. Knarr, N. Stergiou, T.S. Buchanan, A Novel and Safe Approach to Simulate Cutting Movements Using Ground Reaction Forces, *Sensors (Basel)*, 18 (2018) 2631.
- [40] A.S. Lanier, B.A. Knarr, N. Stergiou, L. Snyder-Mackler, T.S. Buchanan, ACL injury and reconstruction affect control of ground reaction forces produced during a novel task that simulates cutting movements, *Journal of orthopaedic research : official publication of the Orthopaedic Research Society*, (2020) 10.1002/jor.24604.
- [41] S.R. Wurdeman, S.A. Myers, N. Stergiou, Transtibial amputee joint motion has increased attractor divergence during walking compared to non-amputee gait, *Annals of biomedical engineering*, 41 (2013) 806-813.
- [42] S.R. Wurdeman, S.A. Myers, A.L. Jacobsen, N. Stergiou, Adaptation and prosthesis effects on stride-to-stride fluctuations in amputee gait, *PLoS One*, 9 (2014) e100125-e100125.

[43] A. Wolf, T. Park, Lyapunov exponent estimation from a time series. Available from: <https://www.mathworks.com/matlabcentral/fileexchange/48084-lyapunov-exponent-estimation-from-a-time-series-documentation-added>, 2016.

## Legends

**Table 1:** Description of the algorithms to calculate EmD, Tau and LyE.

**Table 2:** Recommendations of algorithm and filtering cut off frequency.

**Figure 1:** Power spectral density of the hip, knee and ankle joint angle time series for one representative participants.

**Figure 2:** Flow chart of the data analysis process.

**Figure 3:** Mean  $\pm$  standard error of mean EmD of the hip (black circles), knee (triangles), and ankle (squares) joint angles calculated from the unfiltered (grey) and filtered (black) kinematic data. \* indicates significant difference between EmD of knee joint angle and EmD of the ankle joint angle. \$ indicates significant difference between EmD of hip joint angle and EmD of the knee joint angle. # indicates significant difference between EmD of hip joint angle and EmD of the ankle joint angle.

**Figure 4:** Mean  $\pm$  standard error of mean Tau of the hip (circles), knee (triangles), and ankle (squares) joint angles calculated from the unfiltered (grey) and filtered (black) kinematic data with the five different scripts (in order from the top): Richardson, Richardson128, Stergiou, Stergiou128, and Thomas. \* indicates significant difference between Tau of knee joint angle and Tau of the ankle joint angle. \$ indicates significant difference between Tau of hip joint angle and Tau of the knee joint angle. # indicates significant difference between Tau of hip joint angle and Tau of the ankle joint angle.

**Figure 5:** Mean  $\pm$  standard error of mean LyE of the hip (circles), knee (triangles), and ankle (squares) joint angles calculated from the unfiltered (grey) and filtered (black) kinematic data with the two different algorithms and three different scripts (in order from the top): Rosenstein - Cignetti, Wolf – Knarr, Wolf – Wolf, and Wolf - Wurdeman. \* indicates significant difference between LyE of knee joint angle and LyE of the ankle joint angle. \$ indicates significant difference between LyE of hip joint angle and LyE of

the knee joint angle. # indicates significant difference between LyE of hip joint angle and LyE of the ankle joint angle.

**Table 1:** Description of the algorithms to calculate EmD, Tau and LyE.

Variable	Algorithm script	- Description
EmD	False Nearest Neighbors	It uses a geometrical construction to find nearest neighbors in increasing dimensions of an attractor. When the attractor was determined as being unfolded, then a suitable EmD has been found [34].
	Richardson	A histogram-based method for determining a Tau for phase space reconstruction. Based on the code by Coey and Richardson (2013) [35], which is based on code by Leontitsis [36]. Both used the Sturge's Rule for constructing histograms [37].
Tau	Richardson128	A modification of the Richardson script that uses constant of 128 bins.
	Stergiou	A histogram-based method for determining a Tau for phase space reconstruction. Uses the Scott's equation for constructing histograms [38].
	Stergiou128	A modification of the Stergiou script that uses a constant of 128 bins.
	Thomas	A modification of the code published by Thomas et al. (2014) [22]. The algorithm uses kernel density estimation to determine a Tau for phase space reconstruction.
LyE	Rosenstein – Cignetti	Based on Rosenstein's method for determining LyE [24]. Written by and used by Cignetti et al. (2012) [21]
	Wolf – Knarr	Based on Wolf et al. method for determining LyE [13]. Written by Brian Knarr, this script was revised from the version created by Shane Wurdeman to better utilize MATLAB array operations. It was used in Lanier et al. (2018,2020) [39, 40].
	Wolf – Wurdeman	Based on Wolf's method for determining LyE [13]. Written by Shane Wurdeman and used in Wurdeman et al. (2013,2014) [41, 42].
	Wolf – Wolf	Based on Wolf's method for determining LyE [13]. Written by Wolf and Park (1985) [43].

Note: The Matlab scripts for the Stergiou, Stergiou128 and Wolf-Knarr are available at UNO Biomechanics (2020). UNO Biomechanics Nonlinear Analysis Toolbox (<https://www.mathworks.com/matlabcentral/fileexchange/71907-uno-biomechanics-nonlinear-analysis-toolbox>), MATLAB Central File Exchange.

**Table 2:** Recommendations of algorithm and filtering cut off frequency.

	Recommended computational code/algorithm	Recommended cut off frequency
EmD	False Nearest Neighbors	Unfiltered or > 10Hz
Tau	Richardson128, Stergiou128 or Thomas computational code	Unfiltered or > 10Hz
LyE	Wolf et al. algorithm with the Cignetti, Knarr or Wurdeman computational code	Unfiltered or > 10Hz

**Figure 1:** Power spectral density of the hip, knee and ankle joint angle time series for one representative participants.

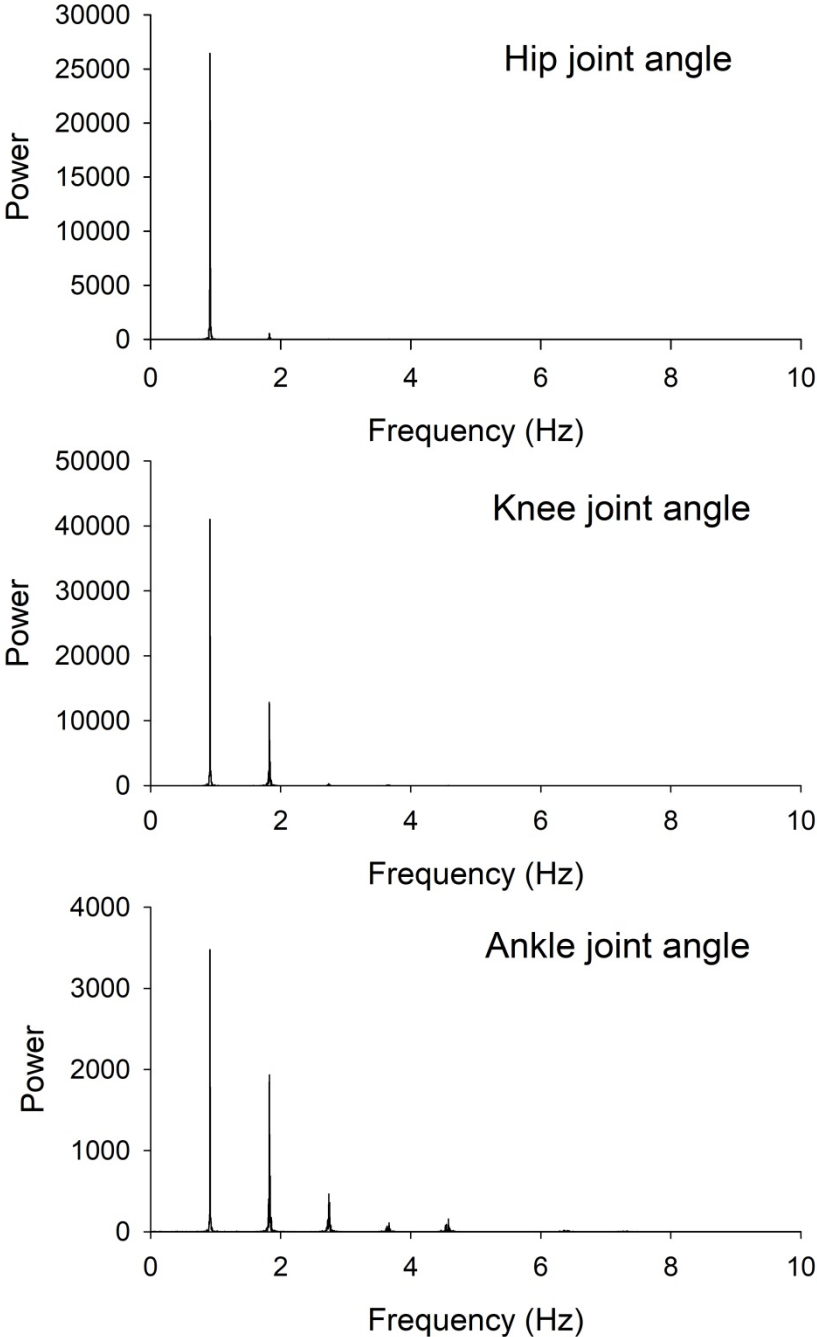


**Figure 2:** Flow chart of the data analysis process.

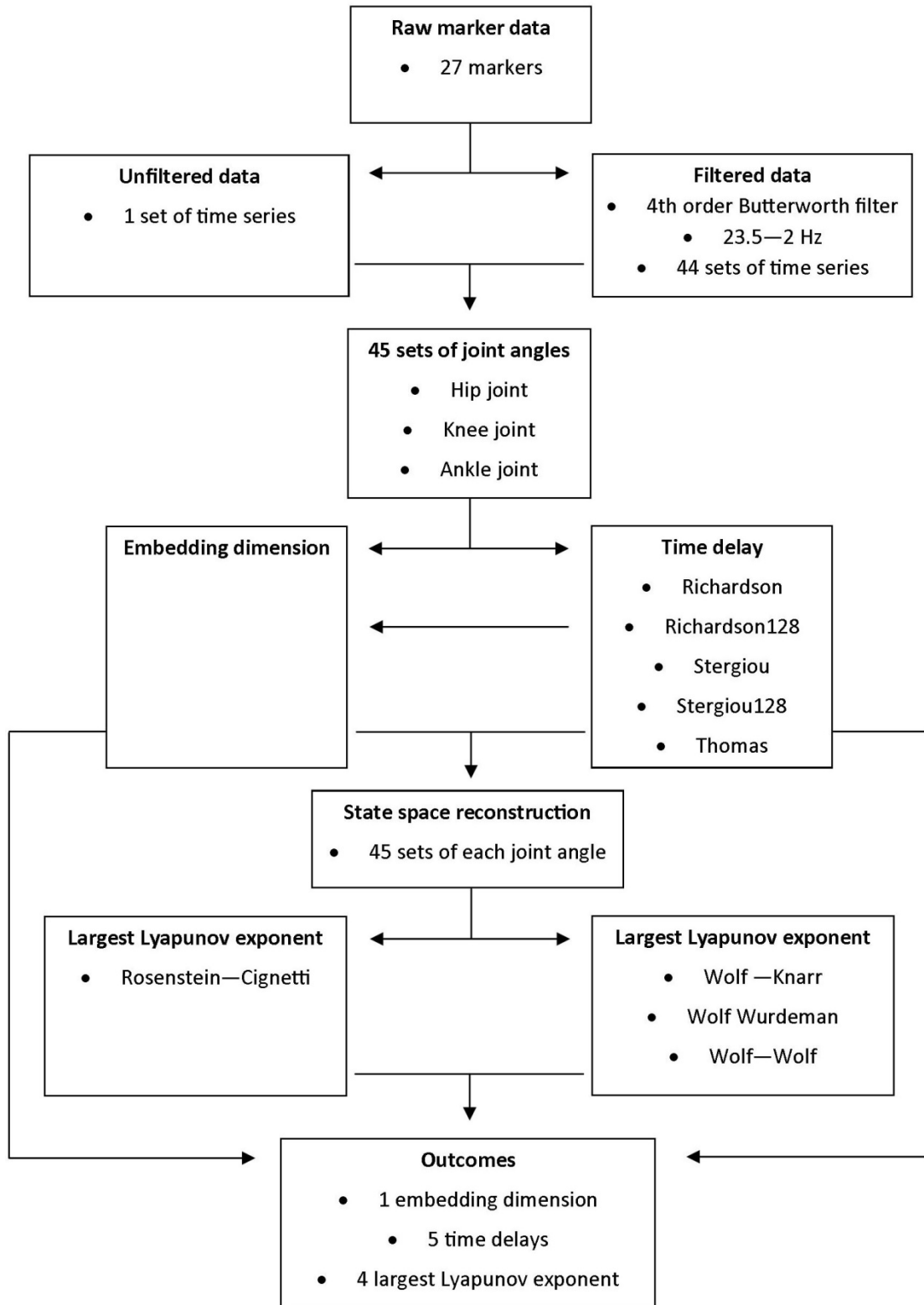


**Figure 3:** Mean  $\pm$  standard error of mean EmD of the hip (black circles), knee (triangles), and ankle (squares) joint angles calculated from the unfiltered (grey) and filtered (black) kinematic data. \* indicates significant difference between EmD of knee joint angle and EmD of the ankle joint angle. \$ indicates significant difference between EmD of hip joint angle and EmD of the knee joint angle. # indicates significant difference between EmD of hip joint angle and EmD of the ankle joint angle.

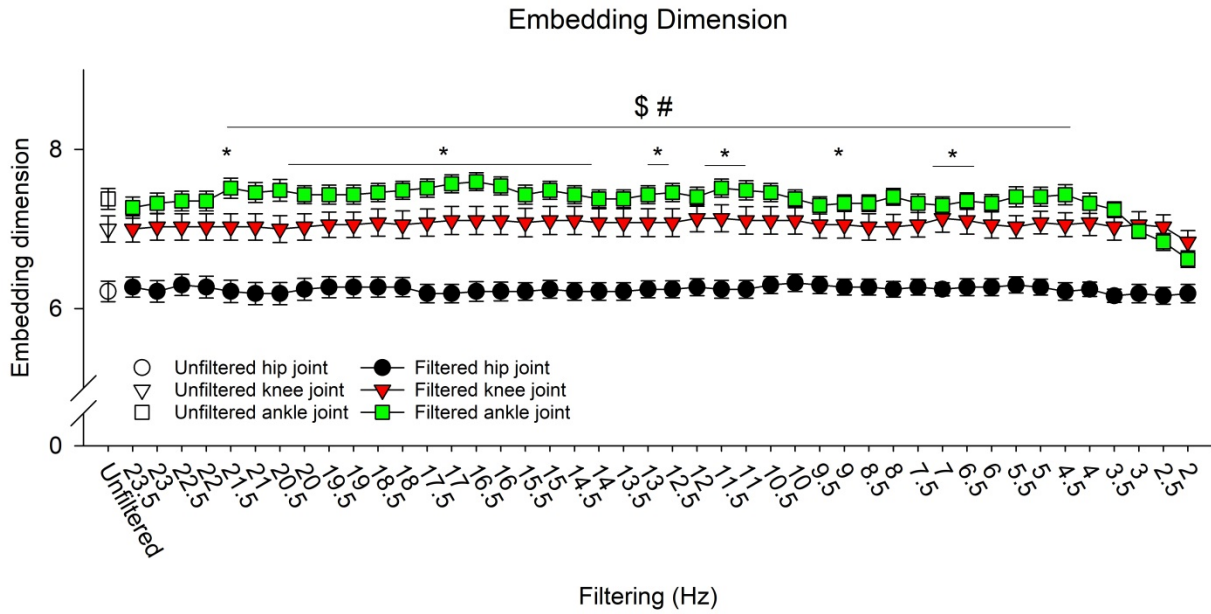


**Figure 4:** Mean  $\pm$  standard error of mean Tau of the hip (circles), knee (triangles), and ankle (squares) joint angles calculated from the unfiltered (grey) and filtered (black) kinematic data with the five different scripts (in order from the top): Richardson, Richardson128, Stergiou, Stergiou128, and Thomas. \* indicates significant difference between Tau of knee joint angle and Tau of the ankle joint angle. \$ indicates significant difference between Tau of hip joint angle and Tau of the knee joint angle. # indicates significant difference between Tau of hip joint angle and Tau of the ankle joint angle.

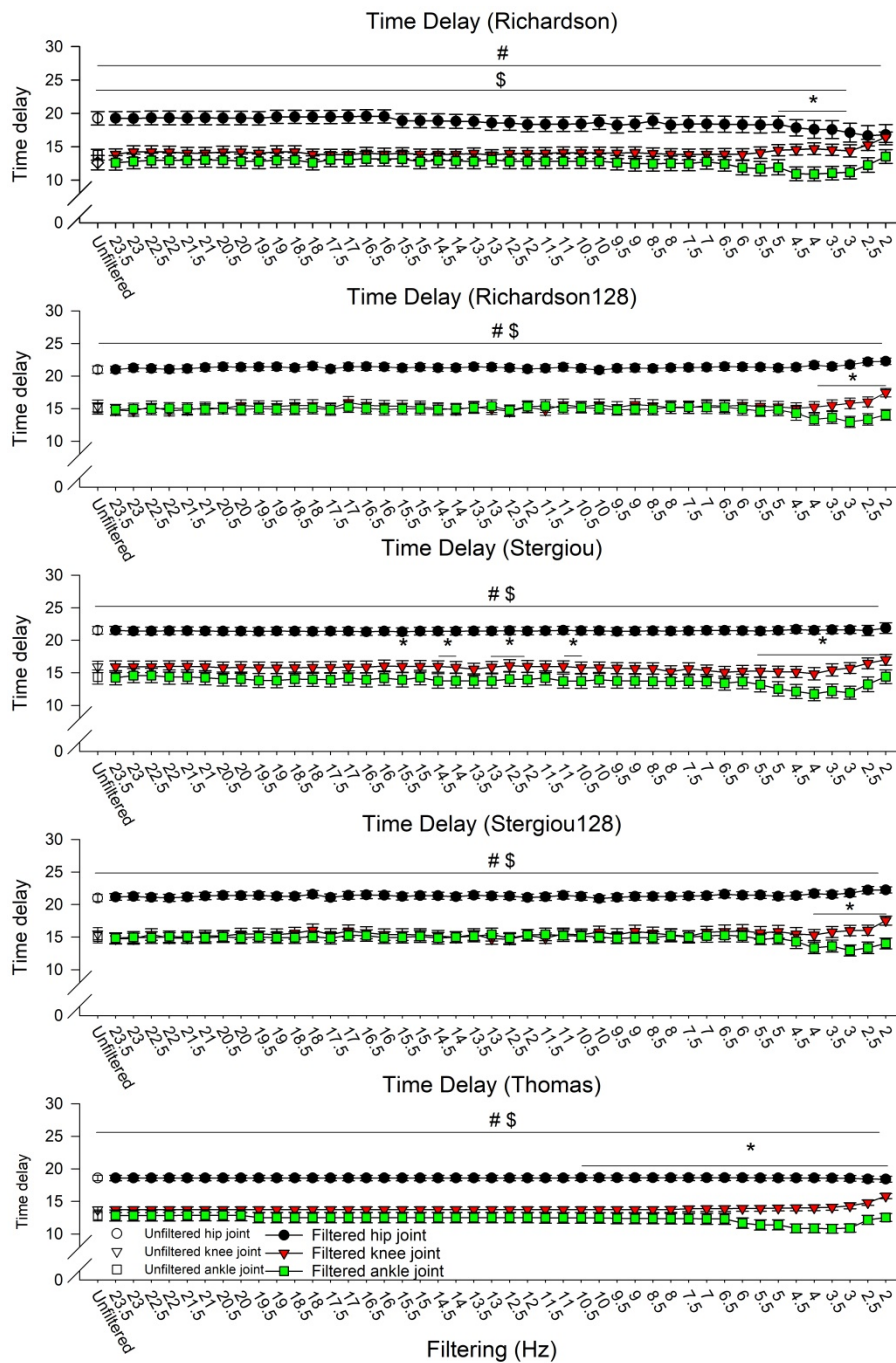


**Figure 5:** Mean  $\pm$  standard error of mean LyE of the hip (circles), knee (triangles), and ankle (squares) joint angles calculated from the unfiltered (grey) and filtered (black) kinematic data with the two different algorithms and three different scripts (in order from the top): Rosenstein - Cignetti, Wolf – Knarr, Wolf – Wolf, and Wolf - Wurdeman. \* indicates significant difference between LyE of knee joint angle and LyE of the ankle joint angle. \$ indicates significant difference between LyE of hip joint angle and LyE of the knee joint angle. # indicates significant difference between LyE of hip joint angle and LyE of the ankle joint angle.

